



HAL
open science

SPIRAL CHOLESTERICs: SURFACE EFFECTS

Michel Mitov, P. Sixou

► **To cite this version:**

Michel Mitov, P. Sixou. SPIRAL CHOLESTERICs: SURFACE EFFECTS. *Modern Physics Letters B*, 1995, 09 (15), pp.929-937. 10.1142/S0217984995000887 . hal-03588870

HAL Id: hal-03588870

<https://hal.science/hal-03588870>

Submitted on 6 Apr 2022

HAL is a multi-disciplinary open access archive for the deposit and dissemination of scientific research documents, whether they are published or not. The documents may come from teaching and research institutions in France or abroad, or from public or private research centers.

L'archive ouverte pluridisciplinaire **HAL**, est destinée au dépôt et à la diffusion de documents scientifiques de niveau recherche, publiés ou non, émanant des établissements d'enseignement et de recherche français ou étrangers, des laboratoires publics ou privés.

SPIRAL CHOLESTERIC: SURFACE EFFECTS

M. MITOV and P. SIXOU

Laboratoire de Physique de la Matière Condensée (u.a. CNRS 190),

Parc Valrose, 06108 Nice, Cedex 2, France

Received 30 November 1994

<https://doi.org/10.1142/S0217984995000887>

The helicoidal structure of the cholesteric phase can be untwisted by the electric field effect. We have shown that spiral-shaped structures could nucleate at the threshold of the field-induced homeotropic state from filaments (linked to the twisted state) embedded in a homeotropic pseudo-nematic matrix (untwisted cholesteric). In this article, we show that confinement and anchoring conditions influence the dynamical behavior and the existence of spiral patterns induced in cholesteric liquid crystals materials by an electric field.

1. Introduction

Spirals are the dominant type of pattern in a remarkable variety of systems: electrohydrodynamical convection,^{1,2} oscillatory chemical reactions,³⁻⁸ biological systems,^{8,9} and are now one of the main themes of nonlinear science. For recent examples, spiral patterns are encountered in thermal convection in a liquid¹⁰ or are currently believed to be responsible for the sudden transition from ventricular tachycardia to fibrillation, leading to sudden death.¹¹ Mechanisms at the origin of these very similar patterns found in very different experimental conditions are not fully understood.

Unwinding of the cholesteric helix by an electric field can be observed in the case of cholesteric liquid crystals with a positive dielectric anisotropy value and an electric field direction perpendicular to the helicoidal axis.¹² In previous papers,^{13,14} we have shown that spirals could germinate from a texture of filaments (linked to the cholesteric phase) embedded in a homeotropic (pseudo-nematic) matrix. The purpose of this letter is to show how the anchoring conditions and the confinement state influence the dynamical behavior of field-induced spirals and can even extinguish the phenomenon.

2. Experimental

The study is made in the case of a mixture between a liquid crystal side-chain polymer (cyclic polysiloxane with two types of mesogens: cholesteric and nematic)¹⁵ and the 5CB nematic liquid crystal (also called K15). The polymer is cholesteric

between 50 and 200°C (left helicity); the pitch is equal to 290 nm (measured near the glassy transition) and the reflection wavelength (at normal incidence) corresponds to the blue of the visible spectrum (450 nm).

Polymer concentration is equal to 9% (in weight); this concentration corresponds to a large pitch cholesteric ($\sim 3 \mu\text{m}$) at ambient temperature (the temperature of the study, which represents an experimental advantage) and up to 42°C. The texture is of fingerprint-type. The sample is contained between two glass plates recovered of a transparent conducting film of I.T.O. (Indium Tin Oxide). The thickness is about $3.5 \mu\text{m}$. Thus, the thickness/natural pitch ratio (confinement ratio) is near to 1: the cell geometry is a confined geometry. We can expect configurations searching to conciliate the natural twisting of the cholesteric structure with the imposed geometric conditions of the cell. The dielectric anisotropy value is +7. The electric field direction is perpendicular to the helicoidal axis which is itself parallel to the cell walls. These conditions lead to an unwinding of the cholesteric structure by the electric field effect.

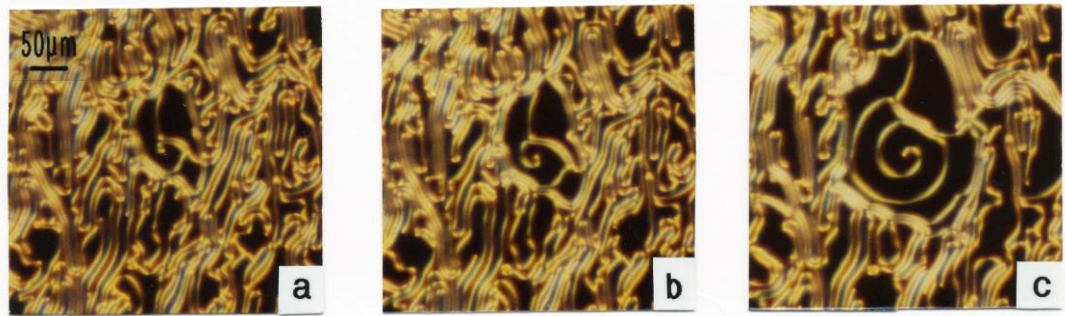


Plate 1. Nucleation and growth of a field-induced spiral-shaped structure from a filament embedded in a homeotropic pseudo-nematic matrix (black zone since observations are made by polarized-light microscopy between crossed polarizers, this zone corresponding to molecules aligned according to the field direction, whether the optic axis). $V = 4.0 \text{ V}$, $f = 50 \text{ Hz}$, Cell thickness = $3.5 \mu\text{m}$, (a) t_0 time. (b) $t_0 + 4 \text{ s}$. (c) $t_0 + 15 \text{ s}$.

3. Results and Discussion

(i) *Influence of field characteristics on the dynamical behavior.* Spiral phenomenon is a threshold phenomenon. It typically occurs for a voltage value between 75% of the threshold voltage value, corresponding to the complete homeotropic state (molecules perpendicular to the surfaces and, thus, parallel to the electric field direction), and the threshold voltage value. In this region, filaments — initially disordered in the homeotropic matrix — are progressively incurving and winding themselves into making spirals (of Archimedian type) of left or right handedness (Plate 1). Nucleation always begins from a fixed point which is a filament extremity. The existence of a state where the homeotropic molecular orientation is a majority is important for the nucleation of spirals as their spreading; if a nucleation center is

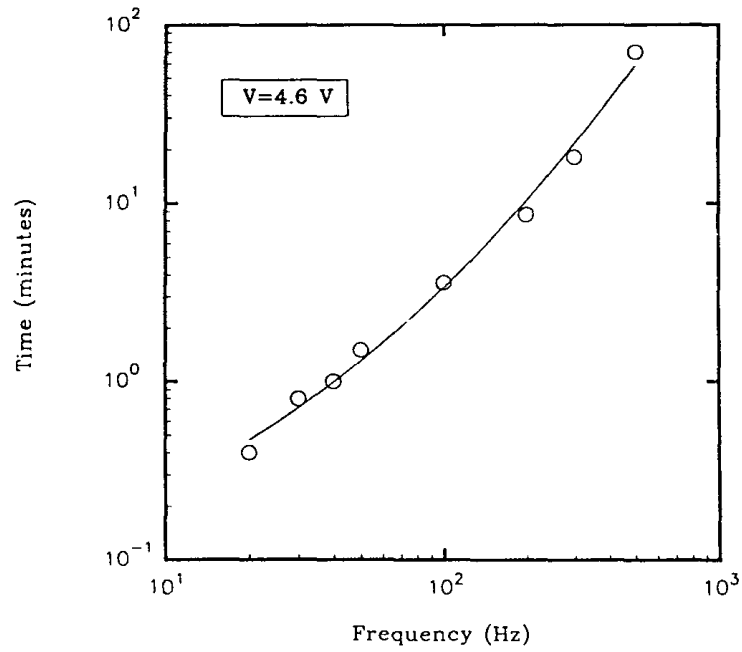


Fig. 1. Nucleation time of a spiral-shaped structure vs frequency (at fixed voltage: 4.6 V). Cell thickness = $3.5 \mu\text{m}$. The initial texture corresponds to filaments (linked to the cholesteric phase) embedded in a homeotropic pseudo-nematic matrix. A spiral nucleates when a filament has described one significant whorl (from a fixed extremity).

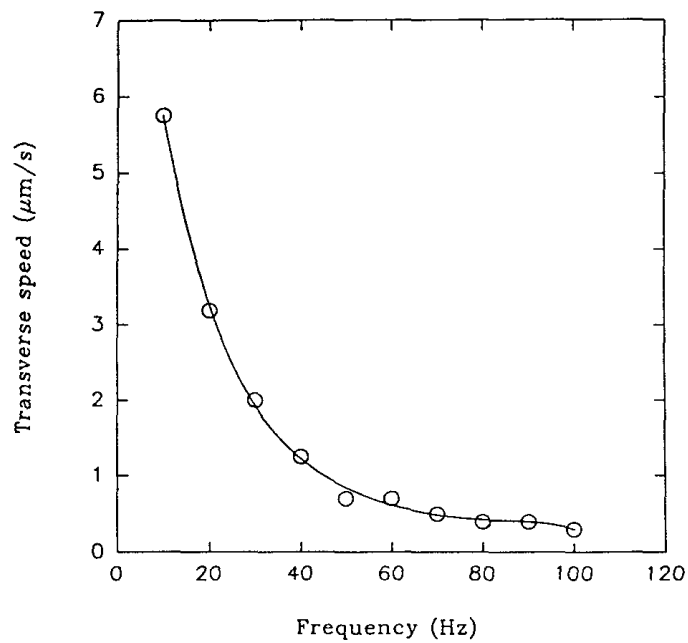


Fig. 2. Transverse speed of a whorl vs frequency (at fixed voltage: 4.6 V). Cell thickness = $3.5 \mu\text{m}$.

surrounded by filaments, the arm of the rising spiral will first release a homeotropic zone around this center and, then, the structure will grow. The frequency value plays a leading part for the nucleation time: if spirals nucleate in less than one minute for frequencies less than 50 Hz, it is necessary to wait long times, more than one hour, as soon as the frequency exceeds 1 kHz (Fig. 1). Thus, nucleation probability is weaker at a high frequency than at a low frequency. For the growth, if we measure the transverse speed of a whorl with respect to frequency, we see that it quickly decreases when frequency increases: typically from 6 to 0.3 $\mu\text{m/s}$ when the frequency varies from 10 to 100 Hz (Fig. 2). A filament spirals up faster at a low frequency than at a high frequency. If the homeotropic state is reached by a too rapid rising in voltage or if the time of observation at the threshold is insufficient with regard to the frequency, the phenomenon can be unperceived. If the observation is followed up after the nucleation of a few spirals, the whole sample is paved with interconnected spirals. It is important to mention that if the field is increased from a configuration exhibiting spirals and non-spiralled filaments, spirals will be the last structures to resist to the homeotropic state propagation.

(ii) *Part of the confinement state.* The confinement state is important for creating optimum observation conditions: for confinement ratios greater than one, the nucleation of spirals is perturbed by convective instabilities which parasite and conceal the observation (Plate 2). On the other hand, the density of spirals is less important when the cholesteric structure is not constrained, the germination being more liable to miscarry.

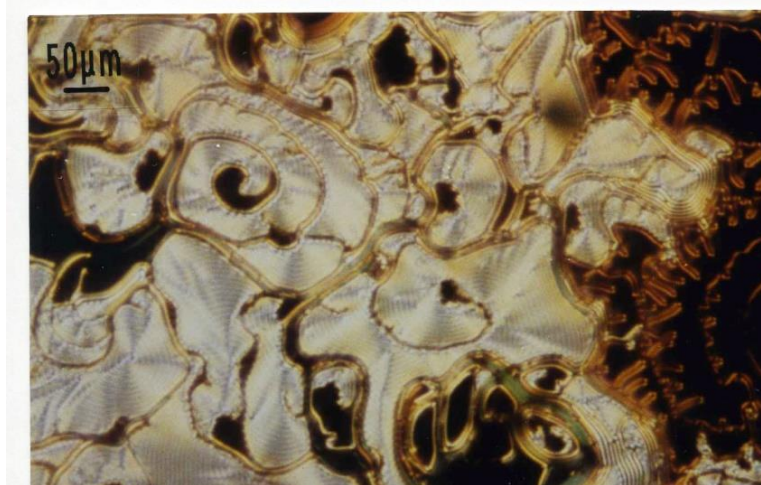


Plate 2. Instabilities (liable to cancel and to parasite the spirals phenomenon). $V = 4 \text{ V}$. $f = 60 \text{ Hz}$.

(iii) *Anchoring influence.* (a) A treatment of cell walls for inducing a strong homeotropic orientation (with a surfactant as ZLI-3124 from Merck or a Linkam cell) does not annihilate the phenomenon but modifies the dynamic comportment. Figure 3 shows the modification of the transverse speed for a whorl in the case of two different anchoring strengths. For a fixed frequency, propagation speed in the

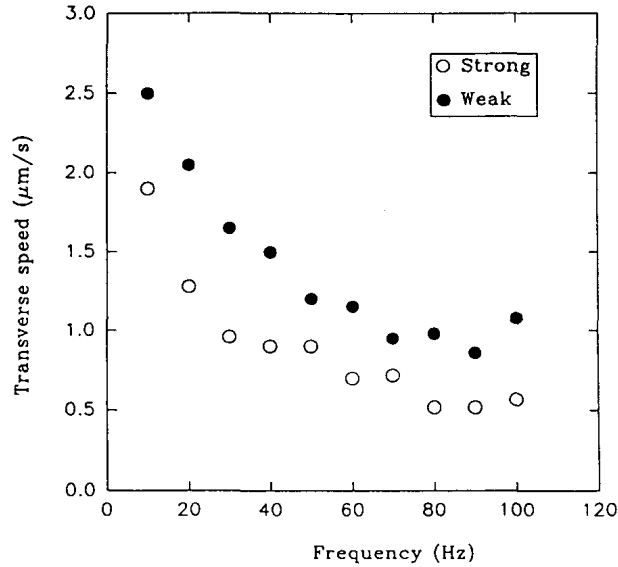


Fig. 3. Transverse speed of a whorl vs frequency (at fixed voltage: 4 V) for two different anchoring strengths. (a) Weak anchoring (I.T.O./liquid crystal interface); cell thickness = 7 μm . (b) Strong anchoring (surfactant/liquid crystal interface); cell thickness = 7.5 μm .

weak anchoring case (I.T.O./liquid crystal interface) is systematically above propagation speed in the strong anchoring case (surfactant/liquid crystal interface). The threshold voltage value is decreased in a strong anchoring case: as we expected 8 V for a thickness of 7.5 μm ¹⁴ we obtain about 5 V (Linkam cell), on account of the induction of the homeotropic orientation (favorable to the dielectric effect) on a more important persistent length. (b) A treatment of cell walls for inducing a planar anchoring (polyamide film) annihilates the spiral nucleation. Cell thickness is 7.5 μm . The structures sequence during the planar to homeotropic transition is as follows (Plate 3). Initially, the texture is uniformly birefringent (any structure or defect can be visualized). Above 2 V, there appears a well-known dielectric instability: the grid-pattern¹⁶; when the dielectric couple tends to re-orient molecules in a configuration corresponding to a fingerprint-type texture, elastic forces tend to preserve the planar configuration. For weak fields, this two-dimensional periodic deformation is an alternative for the director distribution. Between 2 and 3.5 V, the grid periodicity and the birefringence are modified. Above 3.5 V, the fingerprint-type texture is found again; the cholesteric axis has rotated by 90° and is, now, parallel to the cell walls. Then, the cholesteric to homeotropic transition is achieved between 3.5 and 9 V. But no spiral nucleation occurs.

(iv) *Charges injection effect.* An injection of charges by the electrodes¹⁷ can be the cause of space charges formation near the electrodes (in addition to the electrolytic separation mechanism of positive and negative charges). This parasite effect, spe-

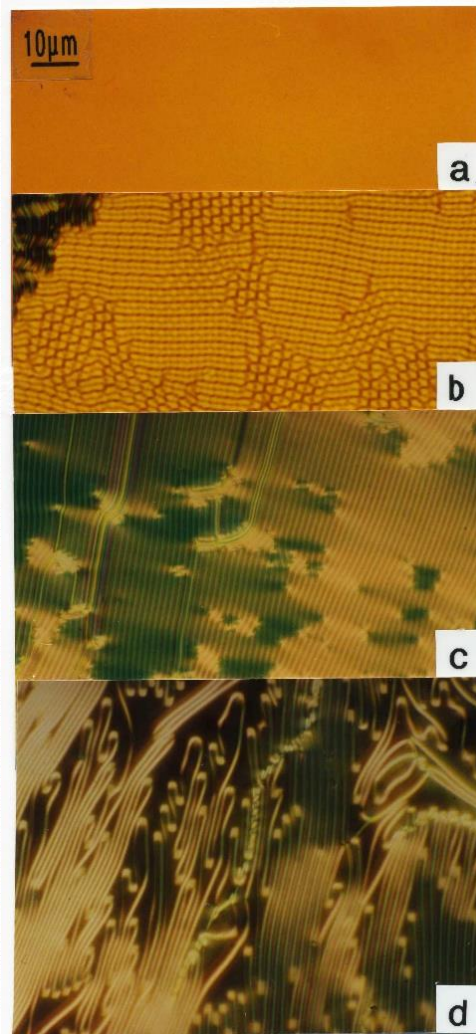


Plate 3. Planar to homeotropic transition. $f = 100$ Hz. Cell thickness = $7.5 \mu\text{m}$. (a) $V = 0$ V. Planar texture. No structure or defect is visible. The cholesteric axis is perpendicular to the picture plane. (b) $V = 2.8$ V. Bi-dimensional deformation (grid-pattern). In the left upper part: nucleation of the fingerprint-type texture. (c) $V = 6.5$ V. Fingerprint-type texture. The cholesteric axis has rotated of 90° . (d) $V = 8$ V. Nucleation of the homeotropic pseudo-nematic state.

cific to the electrodes, is negligible as soon as frequency exceeds some cycles¹⁸ and for small field values. The use of cell walls with an insulating dielectric layer of SiO — of a few hundred angstroms¹⁹ — (and a homeotropic surfactant layer for avoiding the planar anchoring induced by the SiO film) does not annihilate the spiral nucleation.

(v) *Other systems.* Left-handed and right-handed spirals appear when a direct current field is applied to a large pitch cholesteric resulting of mixtures between cholesteric and nematic liquid crystals: 1% of CC (cholesteryl chloride) of CN

(cholesteryl nonanoate) with 89% of MBBA and 10% of 5CB.²⁰ The dielectric anisotropy value is between +1.5 and 2. The CC or CN chiral dopant is used for obtaining a right or left helix sense. This spiral formation is interpreted as the deformation of point singularities formed in the electrode region where there exists an electric field gradient created by the accumulation of injected charges. The handedness of the spiral winding is related to the electrode (cathode or anode) where it is formed. We have reproduced this phenomenon with the mixture: COC (cholesteryl oleyl carbonate, 1%) + MBBA (89%) + 5CB (10%); Plate 4 shows a typical texture. The main difference with respect to our system is that this “screwing” exists for voltages (d.c. fields) clearly inferior to the threshold voltage (≤ 4 V when $V_{th} \sim 7$ V): the homeotropic orientation is a minority. Besides, the extremity of a spiral is not a fixed point: filaments are screwing up until geometric limits of the cell involve a saturation; there is no constant pitch – spiral: a spiral is winding by making its whorls joined. It can initially exist a spiral shape of filaments at the equilibrium (for the fingerprint-type texture) which will be stressed by the field effect. The effect of a field increase (homeotropic propagation) will unwind the so formed spiral, which is different of the dynamical mechanism creating a spiral from a filament embedded in the homeotropic matrix and initially disordered in its pattern.

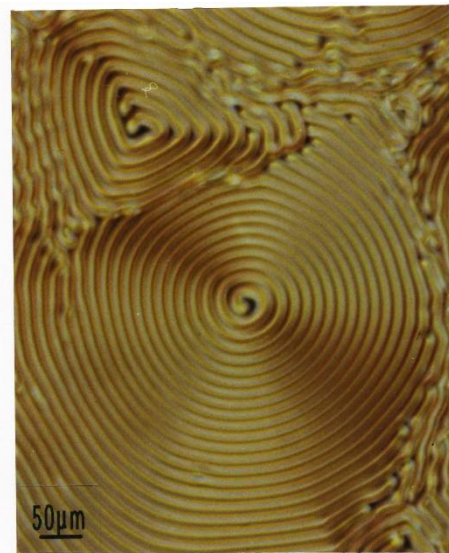


Plate 4. “Screwing” of filaments under a d.c. field (3 V) as in Ref. 20. Mixture: COC (1%) + MBBA (89%) + 5CB (10%). Cell thickness = 16 μm . The core is not a fixed point.

On the other hand, the formation of field-induced spirals from filaments, linked to the cholesteric phase, nucleating in the smectic. A phase, can occur.²¹ The temperature is slowly increased until the smectic A to cholesteric transition tem-

perature occurs (160°C): the cholesteric phase nucleates under a filament pattern with a white tint (corresponding to a low heating rate) and describing as different to the filament pattern observed in literature (see, for example, Refs. 22 and 23); this latter is found again for fast heating rates. Only one type of filaments (white tint) gives rise to spirals. Physical contexts are different: the cholesteric phase coexists with the smectic A phase when only a large pitch cholesteric phase is involved in our system, i.e. far from the smectic A to cholesteric transition (occurring for 35% of polymer at ambient temperature.¹⁴) In the case that we describe, spirals nucleate and grow from filaments embedded in a pseudo-nematic matrix resulting of the untwisting of the cholesteric phase by effect of the electric field: it is only one parameter which permits to achieve the cholesteric to homeotropic nematic transition and to be at the origin of the nucleation and the growth of spirals. Spiral phenomenon is related by the authors to a new phase between smectic A and cholesteric phases analogous with T.G.B. phase. We do not sustain this hypothesis for our system, if only because this context is not ours.

4. Conclusion

In summary, we have shown that frequency, confinement state and anchoring conditions govern the dynamical behavior of field-induced spirals, for the nucleation as the growth, and can even extinguish the phenomenon. The growth seems to be inscribed in a region where the characteristic length (on which are persisting the surface effects) influences the behavior.

The observations being made at the threshold of the homeotropic state, the system is, in a schematic way, marked by the coexistence of two “states” (not in a thermodynamic sense) so we must take intrinsic characteristics into account: a pseudo-nematic state (untwisted cholesteric) concerning the majority of molecules and twisted structures subsisting in the shape of filaments. From this configuration nucleate and grow spiral-shaped structures. One can expect that the chiral doping (at a few percents) of nematic liquid crystal (5CB) does not annihilate mechanisms present in the pure material but rather transposes some of them in electro-optic effects intrinsic to the twisted state. In a next paper we will present a discussion (too long to be included in this letter) about a parallel with electro-optic effects already present in the series of nematic cyanobiphenyls (especially 5CB) based on a mechanism consequent to director deformations near surfaces and propagating within structures where the twist subsists.

References

1. M. Sano, K. Sato, S. Nasuno, and H. Kokubo, *Phys. Rev.* **A46**, 3540 (1992).
2. B. Janiaud, H. Kokubo, and M. Sano, *Phys. Rev.* **E47**, R2237 (1993).
3. S. C. Muller, T. Plessner, and B. Hess, *Science* **230**, 661 (1985).
4. B. F. Madore and W. L. Freedman, *Am. Sci.* **75**, 252 (1987).
5. D. A. Kessler and H. Levine, *Physica* **D39**, 1 (1989).
6. M. Markus and B. Hess, *Nature* **347**, 56 (1990).

7. G. S. Skinner and H. L. Swinney, *Physica* **D48**, 1 (1991).
8. J. J. Tyson and J. P. Keener, *Physica* **D32**, 327 (1988).
9. P. C. Newell and F. M. Ross, *J. Gen. Microbiol.* **128**, 2715 (1982).
10. M. Assenheimer and V. Steinberg, *Nature* **367**, 345 (1994).
11. M. Karma, *Phys. Rev. Lett.* **71**, 7, 1103 (1993).
12. L. M. Blinov, *Electro-optical and magneto-optical properties of liquid crystals* (Wiley, New York, 1983).
13. M. Mitov and P. Sixou, *Mol. Cryst. Liq. Cryst.* **231**, 11 (1993).
14. M. Mitov and P. Sixou, *J. Phys. II*, **2**, 1659 (1992).
15. F.-H. Kreuzer, D. Andrejewski, W. Haas, N. Haberle, G. Riepl, and P. Spes, *Mol. Cryst. Liq. Cryst.* **199**, 345 (1991).
16. See, e.g. W. Helfrich, *Appl. Phys. Lett.* **17**, 531 (1970); F. Rondelez and H. Arnould, *C. R. Acad. Sci.* **B273**, 549 (1971).
17. N. Felici, *Rev. Gen. Electr.* **78**, 17 (1969).
18. F. Rondelez, thesis (Orsay, 1970).
19. We acknowledge P. Barois (C.R.P.P. Pessac) for the insulated electrodes.
20. H. P. Hinov and E. Kukleva, *Mol. Cryst. Liq. Cryst.* **109**, 203 (1984).
21. J.-M. Gilli and M. Kamaye, *Liq. Cryst.* **11**, 791 (1992).
22. (a) M. J. Press and A. S. Arrott, *J. Phys.* **37**, 387 (1976); (b) M. J. Press and A. S. Arrott, *Mol. Cryst. Liq. Cryst.* **37**, 81 (1976).
23. P. Ribière and P. Oswald, *J. Phys. II*, **51**, 1703 (1990).